Ocean Sci. Discuss., https://doi.org/10.5194/os-2018-116
Manuscript under review for journal Ocean Sci.
Discussion started: 1 November 2018

Ocean Science
Discussions
Open Access
EGU

A simple predictive model for the eddy propagation trajectory in the South China Sea

Jiaxun Li[1,2], Guihua Wang[*1], Huijie Xue[3,4], and Huizan Wang[5]

[1]Department of Atmospheric and Oceanic Sciences, Institute of Atmospheric Science, Fudan University, Shanghai, China

[2]Naval Institute of Hydrographic Surveying and Charting, Tianjin, China

[3]State Key Laboratory of Tropical Oceanography, South China Sea Institute of Oceanology, Chinese Academy of Sciences, Guangzhou, China

[4]School of Marine Sciences, University of Maine, Orono, Maine, USA

[5]Institute of Meteorology and Oceanography, National University of Defense Technology, Nanjing, China

Corresponding author: Guihua Wang, Department of Atmospheric and Oceanic Sciences, Institute of Atmospheric Science, Fudan University, Shanghai, China. (wghocean@yahoo.com)

Ocean Sci. Discuss., https://doi.org/10.5194/os-2018-116
Manuscript under review for journal Ocean Sci.
Discussion started: 1 November 2018

Abstract A novel predictive model is built for eddy propagation trajectory using the multiple linear regression method. This simple model has related various oceanic parameters to eddy propagation position changes in the South China Sea (SCS). These oceanic parameters mainly represent the effects of planetary β and mean flow advection on the eddy propagation. The performance of the proposed model is examined in the SCS based on twenty years of satellite altimeter data, and demonstrates its significant forecast skills over a 4-week forecast window comparing to the traditional persistence method. It is also found that the model forecast accuracy is sensitive to eddy polarity and forecast season.

Ocean Sci. Discuss., https://doi.org/10.5194/os-2018-116
Manuscript under review for journal Ocean Sci.
Discussion started: 1 November 2018

1. Introduction

Mesoscale eddies are coherent rotating structures that are ubiquitous over most of the world's oceans (Chelton et al., 2007). They play an important role in the transport of momentum, heat, mass and chemical and biological tracers, thereby become critical for issues such as general circulation, water mass distribution, ocean biology and climate change (Wang et al., 2012; Dong et al., 2014; Zhang et al., 2014; Ma et al., 2016; Li et al., 2017). Therefore, forecasting the eddy propagation positions accurately is not only important scientifically but also important practically for problems such as ocean observing systems designing, fishing planning, and underwater acoustic detecting.

Traditionally, ocean dynamical models were used as the tool of predicting the evolution of ocean eddies (Robinson et al., 1984). To make a useful forecast, accurately updated boundary data, satellite and in situ observation data for assimilation must be available, and a fair degree of computer power is needed (Rienecker et al., 1987; Oey et al., 2005). These restrictions preclude the all-pervading operational use of dynamical models when these initial data and computer power are not feasible due to some reasons.

In this paper, we used a simple statistical method to predict the eddy positions 1-4 weeks in advance using only the past positions of the eddy and its surrounding fields. Our "test block" of ocean is the South China Sea (SCS). It is a semi-enclosed sea under the dramatic influence of the East Asian Monsoon and Kuroshio intrusion (Liu and Xie, 1999; Shaw, 1991). Due to the variable external forcing and complex topography, mesoscale eddies show obvious geographic distributions and various characteristics (Wang et al., 2003; Xiu et al., 2010), but the common character is the overall westward tendency of eddy trajectories no matter of the eddy polarity (Fig. 1). We will first analyze the dynamics of the common westward movement of eddies in the SCS, then develop a simple predictive model of eddy trajectories, and finally

Ocean Sci. Discuss., https://doi.org/10.5194/os-2018-116
Manuscript under review for journal Ocean Sci.
Discussion started: 1 November 2018

discuss the impact of eddy polarity and season on the model forecast accuracy.

2. Data and Methods

2.1 Data

The sea level anomalies (SLA) are from the Archiving, Validation and Interpretation of Satellite Oceanographic data (AVISO, ftp://ftp.aviso.oceanobs.com/) (Ducet et al., 2000). The product merges the measurements of TOPEX/Poseidon, European Remote Sensing Satellite (ERS-1/2), Geosat Follow-on, Jason-1/2, and Envisat, and spans the period from October 14, 1992 to August 7, 2013. Its temporal resolution is weekly, and its spatial resolution is 0.25^{o} latitude by 0.25^{o} longitude. To estimate the large-scale geostrophic currents, we use the absolute dynamic topography (ADT), which consists of the SLAs and a mean dynamic topography (MDT). The method for calculating the MDT was introduced by Rio and Hernandez (2004), and the data is also distributed by AVISO.

The monthly climatology of observed ocean temperature and salinity from U.S. Navy Generalized Digital Environment Model (GDEM-Version 3.0) is used to calculate the phase speed of nondispersive baroclinic Rossby waves in the SCS. It has a horizontal resolution of 0.25^{o} latitude by 0.25^{o} longitude, and 78 standard depths from 0 to 6600 m with the vertical resolution varying from 2 m at the surface to 200 m below 1600 m (Canes, 2009).

The SCS eddy trajectory data is derived from the 3rd release of the global eddy dataset (http://cioss.coas.oregonstate.edu/eddies/). The eddy positions within their trajectories are recorded at 7-day time intervals. A detailed description of the eddy trajectory dataset can be found in Chelton et al. (2011). To forecast the eddy trajectory 1-4 weeks in advance using the last position of the eddy, only eddies with a lifetime of 5 weeks or longer are retained in this study.

Ocean Sci. Discuss., https://doi.org/10.5194/os-2018-116
Manuscript under review for journal Ocean Sci.
Discussion started: 1 November 2018

2.2 Maximum Cross-Correlation Method

The maximum cross-correlation (MCC) method is a space-time lagged technique, which can estimate the surface motions from time-sequential remote sensing images. It has been successfully used to track clouds from geosynchronous satellite data (Leese et al., 1971), to compute sea-ice motion (Ninnis et al., 1986) and advective surface velocities (Emery et al., 1986) from sequential infrared satellite images, and to determine the propagation velocities of ocean eddies from satellite altimeter data (Fu, 2006; Zhuang et al., 2010).

The MCC method mainly consists of two procedures (Fu, 2009): first, the cross-correlations of the SLA time series (h) with others within a certain range box are computed for some time lags (ΔT) in multiples of 7 days (time resolution of SLA data) at each grid node location (x, y) as:

$$C_{x,y}(\Delta x, \Delta y, \Delta T) = \overline{h(x, y, t)h(x+\Delta x, y+\Delta y, t+\Delta T)} \quad (1)$$

where Δx and Δy are the spatial lags and the over bar means time averaging. Second, the position of the maximum correlation at each time lag (ΔT) is identified and a speed can be derived from the time lag and the distance of this position from the origin. Then an average speed vector (u, v) weighted by the correlation coefficients is calculated from the estimates at various time lags as:

$$(u, v) = \frac{\sum_i (\Delta x_i / \Delta T_i, \Delta y_i / \Delta T_i) C_i}{\sum_i C_i} \quad (2)$$

where C_i is the maximum correlation at ΔT_i, and Δx_i, Δy_i are the distances between the position of maximum correlation and the origin. The average velocities are then assigned to the eddy movement velocities at the given grid point. To focus on the mesoscale in the SCS, the time lags are limited to less than 42 days, and the dimension of the search box is generally less than 300 km. To reduce incidental spurious MCC vectors, the maximum speed is set to 30 cm/s, since the phase speeds of baroclinic Rossby waves in the SCS are mostly lower than this threshold (Cai et al., 2008).

Ocean Sci. Discuss., https://doi.org/10.5194/os-2018-116
Manuscript under review for journal Ocean Sci.
Discussion started: 1 November 2018

3. Results

3.1 Dynamics of Eddy Propagation in the SCS

Instead of a Lagrangian description of the movement of individual eddies as reported in the previous studies (e.g., Wang et al., 2003; Chen et al., 2011), the space-time lagged MCC method provides an Eulerian description of the eddy propagation speed. As shown in Fig. 2a and 2d, the MCC method has mapped the propagation speeds of the eddies in the SCS for the winter and summer season, respectively. The propagation of the eddies is generally westward in the ocean interior and southward in the western boundary with the typical speed of 4-10 cm/s. The propagation direction of the eddies generated southwest of Taiwan is southwestward along the 200-2000 m isobaths, indicating the steering effects of the ocean's bathymetry. There are two distinct differences between the winter season and the summer season: one is that the eddy propagation speed in winter is relatively larger than that in summer; and the other is that the influence of the western boundary current can be clearly seen near 16°N-18°N along the Vietnam coast in winter, creating an organized band of southward eddy propagation pattern, while this cannot be found in summer. The different patterns of the eddy propagation speed in winter and summer have revealed several details of the mean flow in the SCS: the large-scale circulation under the influence of northeasterly winter monsoon is stronger than that in the southwesterly summer monsoon, and the robust western boundary current in winter becomes relatively weak and unorganized in summer.

Eddies also have their own westward drift under the planetary β effect in the absence of any mean flow (Nof, 1981, Cushiman-Roisin, 1994). Their propagation speed is approximately the phase speed of the first baroclinic Rossby waves with preferences for small poleward and equatorward deflection of cyclonic and anticyclonic eddies in the global ocean, respectively (Chelton et al., 2007). Theoretically, the phase speed of the first baroclinic Rossby wave is $C_{R1} = -\beta R_1^2$,

Ocean Sci. Discuss., https://doi.org/10.5194/os-2018-116
Manuscript under review for journal Ocean Sci.
Discussion started: 1 November 2018

where the first baroclinic Rossby radius of deformation R_1 is estimated using the climatological GDEM temperature and salinity data. Figure 2b (2e) shows the theoretical phase speed of nondispersive baroclinic Rossby waves calculated from GDEM winter (summer) climatological temperature and salinity data. The direction of the phase speed is due west and the magnitude increases from about 2 cm/s in the north latitude to 12 cm/s in the south latitude.

The differences between the satellite observed propagation speed (Fig. 2a and 2d) and the propagation speed induced by the β effect (Fig. 2b and 2e) in winter and summer are shown in Fig. 2c and 2f, respectively, which may represent the propagation speed caused by the advection of mean flow. To further illustrate the advection effect of mean flow, the winter (summer) mean dynamic topography is superimposed on the propagation speed caused by the mean flow. As can be seen, there is a good spatial correlation (0.61 in the zonal direction and 0.52 in the meridional direction, both of which are significant at the 95% confidence level) between the cyclonic eddy propagation speed advected by the mean flow and the large scale surface cyclonic circulation in winter, both of which are centered northwest of the Luzon Island (Fig. 2c). Due to the weak cyclonic gyre in the northern SCS, the spatial correspondence in summer is not as obvious as that in winter (Fig. 2f). Since the propagation speed induced by the β effect is westward, this tendency is reinforced by the mean flow in the north, but compensated by the mean flow in the south. Because the mean flow in the south is not so strong, it is not able to reverse eddy propagation from its westward motion induced by the β effect as in the Antarctic Circumpolar Current region (Klocker and Marshall, 2014) no matter in winter or summer.

To explore other possible causes of eddy propagation, Fig. 3a shows the annual mean eddy propagation speed. The most striking pattern is that the eddy propagation speed

Ocean Sci. Discuss., https://doi.org/10.5194/os-2018-116
Manuscript under review for journal Ocean Sci.
Discussion started: 1 November 2018

is accelerated markedly on the northern continental shelf of the SCS (also can be seen in Fig. 2a and 2d), corresponding well to the region of negative maximum meridional topographic $\beta_T = \frac{f}{H}\frac{dH}{dy}$, where H is the water depth. Their correlation is -0.40, which is significant at the 95% confidence level. This relatively good correspondence suggests that besides the planetary β effect and advection of mean flow, the topographic β effect also contributes to the eddy propagation in some regions where the bathymetry gradient cannot be neglected.

3.2 Model Development

To develop a simple statistical predictive model for relating various oceanic parameters to eddy propagation position changes, the multiple linear regression is used for developing such statistical forecast models. This method has been successfully used in the forecast of tropical cyclone (TC) tracks (Neumann and Randrianarison, 1976; Aberson and Sampson, 2003), hurricane intensity (Demaria and Kaplan, 1994) and ENSO (Knaff and Landsea, 1997). In this study, the predictands (dependent variables) are the zonal and meridional displacements at each forecast time from the initial position. In choosing the potential predictors (independent variables), two factors are considered. First, the candidates should have a physical link (direct or indirect) with the eddy propagation. Second, the candidates must be available and accessible in advance. Based on these two considerations, eight potential predictors that are associated with eddy propagation are chosen (Table 1). All of these are derived along the eddy trajectories.

These eight predictors can be divided into two categories: 1) those related to climatology and persistence, i.e., “static predictors”, and 2) those related to the changing environmental conditions, i.e., “synoptic predictors”. The static predictors consist of the first six predictors, while the last two are the synoptic predictors. Since the initial eddy position (LON, LAT) and the eddy motion past 1-week (U_PAST,

Ocean Sci. Discuss., https://doi.org/10.5194/os-2018-116
Manuscript under review for journal Ocean Sci.
Discussion started: 1 November 2018

V_PAST) represent the initial conditions of the eddy, these persistence factors are crucial for the next position of the eddy. The climatological eddy zonal and meridional motions (U_CLIM V_CLIM) derived from the MCC method are chosen to take into account the effects of β and the mean flow advection, as discussed in Section 3.1. In reality, the large-scale circulation evolves during the forecast period, but this effect is not taken into account in the climatology and persistence factors. To help account for the time variation of the mean flow advection, the current zonal and meridional absolute geostrophic flows (U_ADT, V_ADT) derived from the satellite data are evaluated at the beginning of the forecast time along the eddy trajectory. The relative contribution of each predictor on each forecast period is illustrated by the normalized regression coefficient (Table 2). To generate the normalized coefficients, both the predictors and the predictands are normalized before they are incorporated into the regression model. The larger the normalized regression coefficient, the greater its contribution to the individual forecast equation. Persistence factors (U_PAST, V_PAST) are initially the most important predictors, while after 2 weeks the most important predictors are the climatology factors (U_CLIM, V_CLIM). The synoptic predictors (U_ADT, V_ADT) contribute less to the forecast equations comparing with persistence and climatology. The underlying reason may be that the week to week variations are too large so the representation of the initial U_ADT and V_ADT to the actual velocities in the 4-week window is not as good as the U_CLIM and V_CLIM.

There are a total of 8 regression equations, i.e., both the meridional and zonal directions for the weeks of 1-4. We can separate the data into two sets: one for regressing and the other for forecasting. At week-1, we used 1981 (76%) eddy trajectory segments (the distances between the eddy positions at 7-day time interval) of 283 eddy trajectories during 1992-2008 for regressing, and 623 (24%) eddy trajectory segments of 81 eddy trajectories during 2009-2013 for forecasting. The other forecast experiments for 2, 3, and 4 weeks maintain the same periods for regressing and forecasting. To evaluate the overall forecast ability of the model, the

Ocean Sci. Discuss., https://doi.org/10.5194/os-2018-116
Manuscript under review for journal Ocean Sci.
Discussion started: 1 November 2018

mean forecast error is defined as the averaged distance (D) between the predicted eddy positions and the satellite observed eddy positions following great circle distance (Ali et al., 2007):

$$D = R \bullet \arccos[\sin Y_o \sin Y_F + \cos Y_o \cos Y_F \cos(X_o - X_F)]$$

where R is the earth radius, X_o (X_F) and Y_o (Y_F) represent the observed (forecast) longitude and latitude in degrees, respectively.

Table 3 lists the number of sampling cases, root-mean-square error (RMSE) and correlation coefficient between the predicted and actual longitudes (latitudes), mean distance errors of our model and persistence method (no change of propagation speed from the initial state, Fig. 4a) over a 4-week horizon. It shows that the developed model beats the persistence method and indicates our model has some forecast skill: the RMSE between the predicted and the actual longitudes (latitudes) throughout the 4-week horizon is 0.33-0.89 (0.30-0.73) degrees with the correlation coefficients >0.93 (>0.95). As an example, Fig. 5 compares the 1-2 weeks forecast performances of our model (blue) and the persistence method (green) with the observation (red). Generally, the eddy trajectory predicted 1-2 weeks in advance by our model coincides well with the observed trajectory with an overall average error of 27.6 km (week-1) and 42.5 km (week-2), and even the convoluted pattern can be reproduced properly (Fig. 5 (right)) though the mean error is slightly larger than the smooth case. In contrast, although the persistence forecast trajectory at week-1 is relatively consistent with the observation (Fig. 5a and 5b), the persistence method cannot forecast the eddy trajectories properly when the forecast horizon increases (Fig. 5c and 5d). This shows the superiority of our forecast model over the persistence method.

3.3 Sensitive Performance of Different Eddy Polarity and Season

Previous studies have shown that anticycloinc eddies and cyclonic eddies in the SCS

Ocean Sci. Discuss., https://doi.org/10.5194/os-2018-116
Manuscript under review for journal Ocean Sci.
Discussion started: 1 November 2018

have different dynamic characteristics, such as generation sites, rotation speeds and propagation trajectories, and the seasonal variability of these eddies is robust (Wang et al., 2006; Wang et al., 2008; Li et al., 2011). Two natural questions arise: 1) is there any difference on the model forecast ability between anticyclonic eddies (Fig. 1a) and cyclonic eddies (Fig. 1b)? 2) If so, is there any difference on the forecast ability for one type of eddies in winter (Fig. 6a and 7a) and summer (Fig. 6b and 7b)? This section will explore the different model performances on two types of eddies and during different seasons in the SCS.

The period considered for regressing and predicting the anticyclonic eddy and cyclonic eddy positions is the same as that used in developing the predictive model in Section 3.2. The mean forecast errors of anticyclonic (cyclonic) eddies from week-1 to week-4 are 36.9 km (41.1 km), 62.6 km (68.1 km), 81.0 km (88.5 km), and 102.0 km (108.2 km), respectively (Fig. 1c). These results show that the predicted trajectory errors of anticyclonic eddies are less than those of cyclonic eddies in all forecast horizon, and the maximum error difference can reach 7.5 km at week-3. To investigate the underlying reasons of different model performances for anticyclonic eddies and cyclonic eddies, we use the persistence error ($CC' = \sqrt{AB^2 + BC^2 - 2AB \bullet BC \bullet \cos\theta}$ in Fig. 4a) at week-1 as an index to measure the difficulty of trajectory forecast. The underlying reason in physics is that CC', which includes the effects of winding angel (θ, measuring the trajectory curvature) and the eddy propagation distances in the former and latter periods (AB and BC, measuring the eddy propagation speed), is an integral characteristic of eddy trajectory. The correlation between this integrated index and eddy trajectory forecast error is relatively high with R=0.62, which is significant at the 95% confidence level and shows its ability of measuring the inherent difficulty of trajectory forecast: the larger the index, the more difficult the trajectory forecast, thus the larger the forecast error. Because the indices (mean persistence errors) of all the anticyclonic and cyclonic eddy trajectories in the SCS are 46.6 km and 53.0 km, respectively, it is not difficult to understand why the mean forecast error of

Ocean Sci. Discuss., https://doi.org/10.5194/os-2018-116
Manuscript under review for journal Ocean Sci.
Discussion started: 1 November 2018

anticyclonic eddy trajectories is smaller than that of cyclonic eddy trajectories in the SCS. The index difference between anticyclonic and cyclonic eddy trajectories is caused by these different trajectory patterns (Fig. 1a and 1b), which could be due to the opposing meridional drifts of anticyclonic and cyclonic eddies expected from the combination of β effect and self-advection (Morrow et al., 2004).

Figure 6c (Fig. 7c) shows the mean forecast errors of anticyclonic (cyclonic) eddy trajectories in winter and summer over a 4-week horizon. Because the mean persistence error (42.0 km) of anticyclonic eddy trajectories in winter is smaller than that (51.9 km) in summer, as expected, the mean forecast error of anticyclonic eddy trajectories in winter is smaller than that in summer for all cases. This is also the case for the cyclonic eddy: since the mean persistence error (54.6 km) of cyclonic eddy trajectories in winter is relatively larger than that (52.8 km) in summer, the mean forecast error of cyclonic eddy trajectories in winter is larger than that in summer. The index difference of one type of eddy trajectories between winter and summer is also caused by the different trajectory patterns. Why do the anticyclonic and cyclonic eddies follow different trajectories in winter (Fig. 6a and 7a) and summer (Fig. 6b and 7b)? One possible dynamical reason is the different interactions between the eddies and seasonal mean flows. Other underlying factors such as eddy generation mechanisms and eddy-topography interactions in different seasons may also contribute. This is beyond the scope of this study and needs further investigation using numerical models.

4. Summary and Discussion

In this study we have investigated the underlying dynamics of the eddy propagation in the SCS and found the propagation of SCS eddies is mainly driven by the combination of the planetary β effect and mean flow. In addition, the topographic β effect also has some contribution to the eddy propagation where the bathymetry gradient cannot be neglected, like the steep continental shelf in the northern SCS (Fig.

Ocean Sci. Discuss., https://doi.org/10.5194/os-2018-116
Manuscript under review for journal Ocean Sci.
Discussion started: 1 November 2018

309 1a).

310

311 Based on the dynamical analysis, a simple statistical predictive model for relating
312 various oceanic parameters to eddy propagation position changes is developed using
313 the multiple linear regression method. This model is made up of two predictands
314 (zonal and meridional displacements) and eight predictors (six static predictors, two
315 synoptic predictors). The six static predictors are associated with the initial position,
316 the zonal and meridional motions past 1-week, and the climatological eddy zonal and
317 meridional motion. The other two synoptic predictors account for the time variation of
318 the mean flow advection. Results showed that this simple model has significant
319 forecast skills over a 4-week forecast horizon comparing the traditional persistence
320 method. Moreover, the model performance is sensitive to eddy type and forecast
321 season: 1) the predicted trajectory errors of anticyclonic eddies are smaller than those
322 of cyclonic eddies; 2) the predicted trajectory errors of anticyclonic eddies in winter
323 are smaller than those in summer; while the contrary is the case for the cyclonic eddy.
324 The predictive model performance strongly depends on the inherent difficulty of
325 trajectory forecast.

326

327 Although the performance of the proposed predictive model is encouraging, it could
328 be refined further. Further improvement may be possible by including the effect of
329 eddy-eddy interactions on the eddy propagation, which is supposed to help induce the
330 eddy trajectory curve or loop (Early et al., 2011). Another possible improvement is to
331 replace the multiple regression method with machine learning (ML) techniques.
332 Ashkezari et al. (2016) have shown that the ML methods particularly stand out in
333 analyzing complex systems yet not fully understood, like estimating the eddy lifetime.
334 These enhancements are topics warranting future research and development.

335

336

337 *Data availability.* The SLA and MDT data can be downloaded from AVISO
338 (ftp://ftp.aviso.oceanobs.com/), and the SCS eddy trajectory data can be derived from
339 the 3rd release global eddy dataset (http://cioss.coas.oregonstate.edu/eddies/).
340

341 *Acknowledgements.* This work is supported by the National Key Research and
342 Development Program of China (2017YFC1404103), the National Basic Research
343 Program of China (2013CB430301), the Natural Science Foundation of China
344 (91428206, 41621064, 91528304), the National Programme on Global Change and
345 Air-Sea Interaction (GASIIPOVAI-04), and the China Postdoctoral Science
346 Foundation (2016M601493).
347

348 ## References

349 Aberson, S. D. and Sampson, C. R.: On the predictability of tropical cyclone tracks in the
350 northwest pacific basin, Mon. Wea. Rev., 131, 1491-1497, 2003.
351 Ali, M. M., Kishtawal, C. M., and Jain, S.: Predicting cyclone tracks in the north Indian Ocean:
352 An artificial neural network approach, Geophys. Res. Lett., 34, L04603,
353 http://doi.org/10.1029/2006GL028353, 2007.
354 Ashkezari, M. D., Hill, C. N., Follett, C. N., Forget, G., and Follows, M. J.: Oceanic eddy
355 detection and lifetime forecast using machine learning methods, Geophys. Res.
356 Lett., 43, 12,234–12,241, http://doi.org/10.1002/2016GL071269, 2016.
357 Cai, S., Long, X., Wu, R., and Wang, S.: Geographical and monthly variability of the first
358 baroclinic rossby radius of deformation in the south china sea, J. Mar. Syst., 74, 711-720, 2008.
359 Canes, M. R.: Description and evaluation of GDEM-V3.0, Rep.NRL/MR/7330-09-9165, Nav. Res.
360 Lab, Washington, D. C, 2009.
361 Chelton, D. B., Schlax, M. G., and Samelson, R. M.: Global observations of nonlinear mesoscale
362 eddies, Prog. Oceanogr., 91, 167-216, 2011.
363 Chelton, D. B., Schlax, M. G., Samelson, R. M., and de Szoeke, R. A.: Global observations of
364 large oceanic eddies, Geophys. Res. Lett., 34, L15606, http://doi.org/10.1029/2007GL030812,

2007.

Chen, G., Hou, Y., and Chu, X.: Mesoscale eddies in the South China Sea: Mean properties, spatiotemporal variability, and impact on thermohaline structure, J. Geophys. Res., 116, C06018, http://doi.org/10.1029/2010JC006716, 2011.

Cushiman-Roisin, B.: Introduction to Geophysical Fluid Dynamics, Prentice Hall, 320 pp, 1994.

Demaria, M. and Kaplan, J.: A statistical hurricane intensity prediction scheme (SHIPS) for the Atlantic basin, Weather Forecast, 9, 209-220, 1994.

Dong, C., Mcwilliams, J. C., Liu, Y., and Chen, D.: Global heat and salt transports by eddy movement, Nature Communications, 5, 3294, 2014.

Ducet, N., Le Traon, P. Y., and Reverdin, G.: Global high-resolution mapping of ocean circulation from TOPEX/Poseidon and ERS-1 and -2, J. Geophys. Res., 105, 19477–19498, http://doi.org/10.1029/2000JC900063, 2000.

Early, J. J., Samelson, R. M., and Chelton, D. B.: The evolution and propagation of quasigeostrophic ocean eddies, J. Phys. Oceanogr., 41, 1535-1555, 2011.

Emery, W. J., Thomas, A. C., Collins, M. J., Crawford, W. R., and Mackas, D. L.: An objective method for computing advective surface velocities from sequential infrared satellite images, J. Geophys. Res., 91, 12865–12878, http://doi.org/ 10.1029/JC091iC11p12865, 1986.

Fu, L.-L.: Pathways of eddies in the South Atlantic Ocean revealed from satellite altimeter observations, Geophys. Res. Lett., 33, L14610, http://doi.org/10.1029/2006GL026245, 2006.

Fu, L.-L.: Pattern and speed of propagation of the global ocean eddy variability, J. Geophys. Res., 114, C11017, http://doi.org/10.1029/2009JC005349, 2009.

Klocker, A. and Marshall, D. P.: Advection of baroclinic eddies by depth mean flow, Geophys. Res. Lett., 41, 3517–3521, http://doi.org/10.1002/2014GL060001, 2014.

Knaff, J. A. and Landsea, C. W.: An El Nino-Southern Oscillation climatology and persistence (CLIPER) forecasting scheme, Weather Forecast, 12, 633-652, 1997.

Leese, J. A., Novak, C. S., and Clark, B. B.: An automated technique for obtaining cloud motion from geosynchronous satellite data using cross correlation, J. Appl. Meteor., 10, 18-132, 1971.

Li, J., Zhang, R., and Jin, B.: Eddy characteristics in the northern South China Sea as inferred from Lagrangian drifter data, Ocean Sci., 7, 1575-1599, 2011.

Li, J., Wang, G., and Zhai, X.: Observed cold filaments associated with mesoscale eddies in the

Ocean Sci. Discuss., https://doi.org/10.5194/os-2018-116
Manuscript under review for journal Ocean Sci.
Discussion started: 1 November 2018

South China Sea, J. Geophys. Res. Oceans, 122, 762–770, http://doi.org/10.1002/2016JC012353, 2017.

Liu, W. T. and Xie, X.: Space-based observations of the seasonal changes of South Asian monsoons and oceanic response, Geophys. Res. Lett., 26, 1473-1476, 1999.

Ma, X. and Coauthors: Western boundary currents regulated by interaction between ocean eddies and the atmosphere, Nature, 535, 533, 2016.

Morrow, R., Birol, F., Griffin, D., and Sudre, J.: Divergent pathways of cyclonic and anti-cyclonic ocean eddies, Geophys. Res. Lett., 31, L24311, http://doi.org/10.1029/2004GL020974, 2004.

Neumann, C. J. and Randrianarison, E. A.: Statistical prediction of tropical cyclone motion over the southwest indian ocean, Mon. Wea. Rev., 104, 76-85, 1976.

Ninnis, R. M., Emery, W. J., and Collins, M. J.: Automated extraction of pack ice motion from advanced very high resolution radiometer imagery, J. Geophys. Res., 91, 10725–10734, http://doi.org/10.1029/JC091iC09p10725, 1986.

Nof, D.: On the β-induced movement of isolated baroclinic eddies, J. Phys. Oceanogr., 11, 1662-1672, 1981.

Oey, L.-Y., Ezer, T., Forristall, G., Cooper, C., DiMarco, S., and Fan, S.: An exercise in forecasting loop current and eddy frontal positions in the Gulf of Mexico, Geophys. Res. Lett., 32, L12611, http://doi.org/10.1029/2005GL023253, 2005.

Rienecker, M. M., Mooers, C. N. K., and Robinson, A. R.: Dynamical interpolation and forecast of the evolution of mesoscale features off northern California, J. Phys. Oceanogr., 17, 1189-1213, 1987.

Rio, M.-H. and Hernandez, F.: A mean dynamic topography computed over the world ocean from altimetry, in situ measurements, and a geoid model, J. Geophys. Res., 109, C12032, http://doi.org/10.1029/2003JC002226, 2004.

Robinson, A. R., Carton, J. A., Mooers, C. N. K., Walstad, L. J., Carter, E. F., Rienecker, M. M., Smith, J. A., and Leslie, W. G.: A real-time dynamical forecast of ocean synoptic/mesoscale eddies, Nature, 309, 781-783, 1984.

Shaw, P. T.: Seasonal variation of the intrusion of the Philippine Sea water into the South China Sea, J. Geophys. Res., 96, 821-827, 1991.

Wang, G., Su, J., and Chu, P. C.: Mesoscale eddies in the South China Sea observed with altimeter

425 data, Geophys. Res. Lett., 30, 2121, http://doi.org/10.1029/2003GL018532, 21, 2003.
426 Wang, G., Chen, D., and Su, J.: Generation and life cycle of the dipole in the South China Sea
427 summer circulation, J. Geophys. Res., 111, C06002, http://doi.org/10.1029/2005JC003314,
428 2006.
429 Wang, G., Chen, D., and Su, J.: Winter eddy genesis in the eastern South China Sea due to
430 orographic wind-jets, J. Phys. Oceanogr., 38, 726–732, http://doi.org/10.1175/2007JPO3868.1,
431 2008.
432 Wang, G., Li, J., Wang, C., and Yan, Y.: Interactions among the winter monsoon, ocean eddy and
433 ocean thermal front in the South China Sea, J. Geophys. Res., 117, C08002,
434 http://doi.org/10.1029/2012JC008007, 2012.
435 Zhuang W., Du, Y., Wang, D., Xie, Q., and Xie, S.-P.: Pathways of mesoscale variability in the
436 South China Sea, Chin. J. Oceanol. Limnol., 28, 1055-1067, 2010.
437 Xiu, P., Chai F., Shi, L., Xue, H., and Chao, Y.: A census of eddy activities in the South China Sea
438 during 1993–2007, J. Geophys. Res., 115, C03012, http://doi.org/10.1029/2009JC005657, 2010.
439 Zhang, Z., Wang, W., and Qiu, B.: Oceanic mass transport by mesoscale eddies, Science, 345, 322,
440 2014.
441

Ocean Sci. Discuss., https://doi.org/10.5194/os-2018-116
Manuscript under review for journal Ocean Sci.
Discussion started: 1 November 2018

442 **Figure and Table Captions**

443 **Figure 1.** The trajectories of (a) anticyclonic and (b) cyclonic eddies with lifetime ≥ 5
444 weeks in the South China Sea (SCS). The solid circle represents the ending position
445 of each trajectory. In Fig. 1a, TI: Taiwan Island, LI: Luzon Islands, VN: Vietnam. The
446 two isobaths are for 200 m and 2000 m, respectively. (c) Comparison of the mean
447 forecast errors between anticyclonic eddies (red) and cyclonic eddies (blue) over a
448 4-week window.

449

450 **Figure 2.** Winter climatology of (a) eddy propagation speed directions (vectors) and
451 magnitudes (color, cm/s), (b) The phase speed directions (vectors) and magnitudes
452 (color, cm/s) of the first baroclinic Rossby wave. (c) The speed difference (vectors)
453 between (a) and (b) superimposed on the winter mean absolute dynamic topography
454 (color, cm). (d), (e) and (f) are the same as (a), (b) and (c), respectively, but for the
455 summer.

456

457 **Figure 3.** (a) Annual mean of eddy propagation speed directions (vectors) and
458 magnitudes (color, cm/s). (b) Meridional distribution of the topographic β effect
459 (color shading).

460

461 **Figure 4.** (a) Schematic of persistence method. A, B, and C are three observed eddy
462 positions on the trajectory every 1 week interval. C' is the predictive eddy position 1
463 week in advance by persistence method, that is BC'=AB. Thus CC' is the persistence
464 error at week-1. (b) Scatterplot of persistence error versus forecast error of our model
465 at week-1 with best fit linear regression.

466

467 **Figure 5.** A comparison of the satellite observed trajectory (red), the predicted
468 trajectory by our model (blue) and persistence trajectory (green) at (a) week-1, (c)
469 week-2. (b), (d) are the same as (a) and (c), respectively, but for a recurved trajectory.
470 The biweekly eddy positions on each trajectory are shown by the solid circles.

Ocean Sci. Discuss., https://doi.org/10.5194/os-2018-116
Manuscript under review for journal Ocean Sci.
Discussion started: 1 November 2018

Figure 6. The trajectories of anticyclonic eddies in (a) winter and (b) summer with lifetime ≥ 5 weeks in the South China Sea (SCS). The solid circle represents the ending position of each trajectory. (c) Comparison of their mean forecast errors over a 4-week window.

Figure 7. The same as Fig. 6, but for the cyclonic eddies.

Table 1. The Eight Predictors Used in the Predictive Model.

Table 2. Normalized Regression Coefficients for Use with the Eddy Zonal (Meridional) Motion Prediction Equation.

Table 3. Statistics of our Predictive Model for Different Forecast Time of Eddy Propagation Positions in Terms of Longitudes (Latitudes).

Ocean Sci. Discuss., https://doi.org/10.5194/os-2018-116
Manuscript under review for journal Ocean Sci.
Discussion started: 1 November 2018

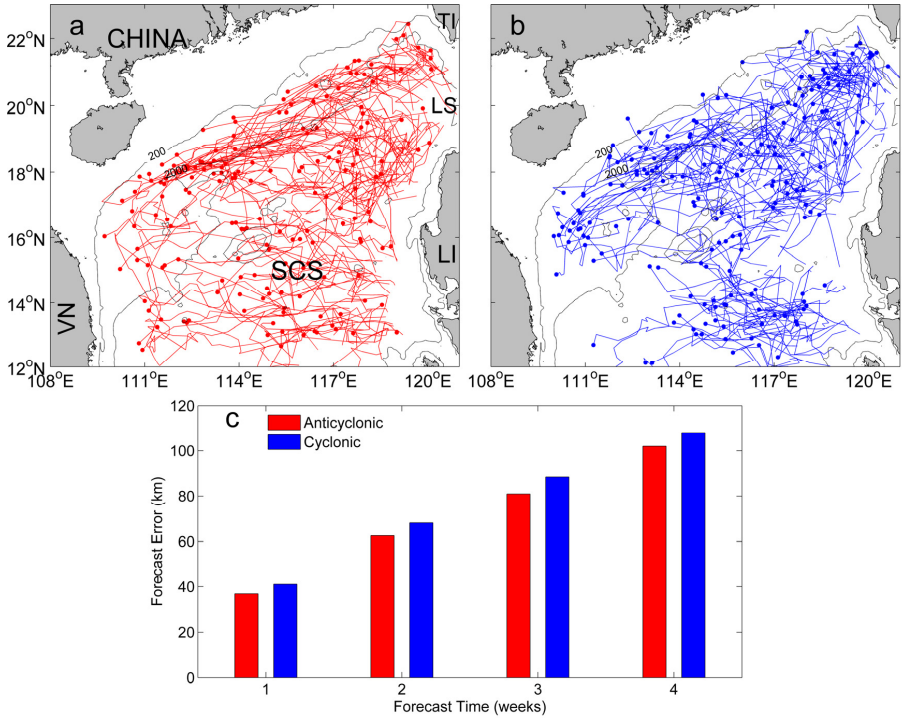

Figure 1. The trajectories of (a) anticyclonic and (b) cyclonic eddies with lifetime ≥ 5 weeks in the South China Sea (SCS). The solid circle represents the ending position of each trajectory. In Fig. 1a, TI: Taiwan Island, LI: Luzon Islands, VN: Vietnam. The two isobaths are for 200 m and 2000 m, respectively. (c) Comparison of the mean forecast errors between anticyclonic eddies (red) and cyclonic eddies (blue) over a 4-week window.

Ocean Sci. Discuss., https://doi.org/10.5194/os-2018-116
Manuscript under review for journal Ocean Sci.
Discussion started: 1 November 2018

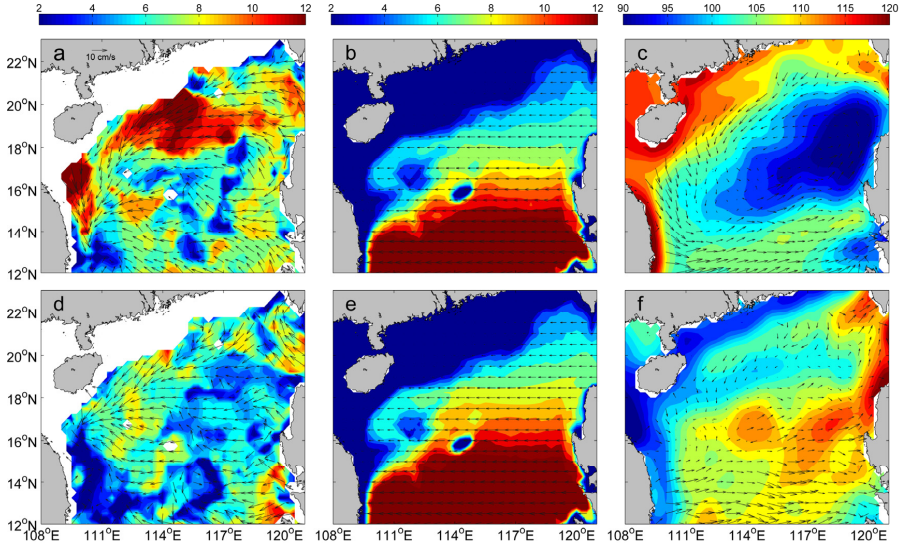

Figure 2. Winter climatology of (a) eddy propagation speed directions (vectors) and magnitudes (color, cm/s), (b) The phase speed directions (vectors) and magnitudes (color, cm/s) of the first baroclinic Rossby wave. (c) The speed difference (vectors) between (a) and (b) superimposed on the winter mean absolute dynamic topography (color, cm). (d), (e) and (f) are the same as (a), (b) and (c), respectively, but for the summer.

Ocean Sci. Discuss., https://doi.org/10.5194/os-2018-116
Manuscript under review for journal Ocean Sci.
Discussion started: 1 November 2018

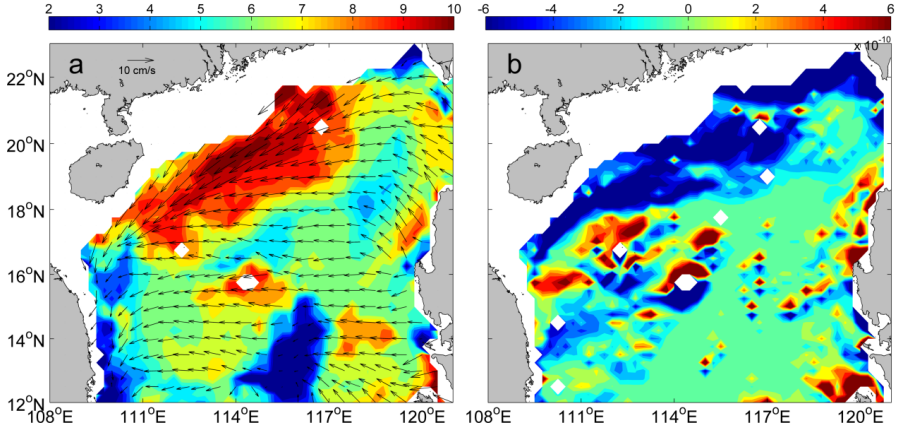

505
506

507 **Figure 3.** (a) Annual mean of eddy propagation speed directions (vectors) and
508 magnitudes (color, cm/s). (b) Meridional distribution of the topographic β effect
509 (color shading).

510

Ocean Sci. Discuss., https://doi.org/10.5194/os-2018-116
Manuscript under review for journal Ocean Sci.
Discussion started: 1 November 2018

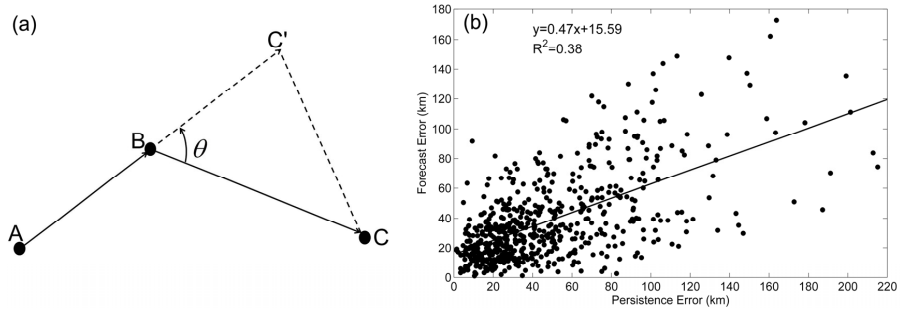

Figure 4. (a) Schematic of persistence method. A, B, and C are three observed eddy positions on the trajectory every 1 week interval. C' is the predictive eddy position 1 week in advance by persistence method, that is BC'=AB. Thus CC' is the persistence error at week-1. (b) Scatterplot of persistence error versus forecast error of our model at week-1 with best fit linear regression.

Ocean Sci. Discuss., https://doi.org/10.5194/os-2018-116
Manuscript under review for journal Ocean Sci.
Discussion started: 1 November 2018

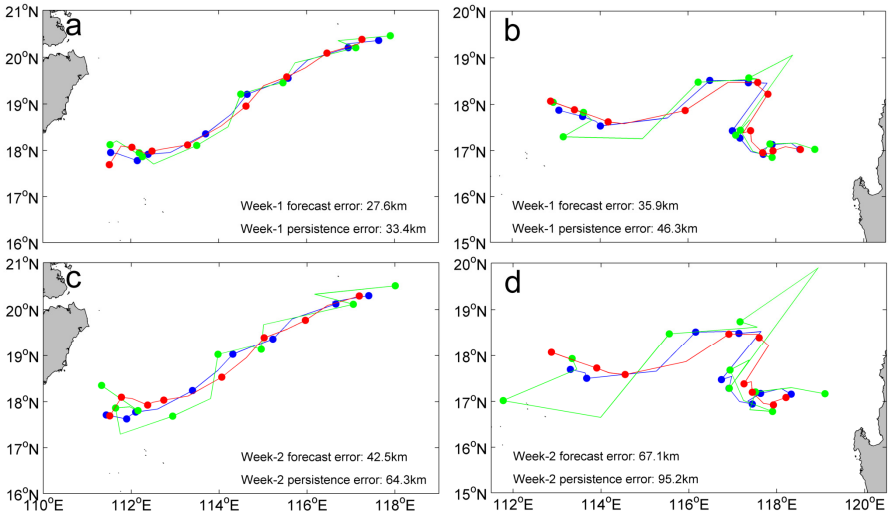

519
520

521 **Figure 5.** A comparison of the satellite observed trajectory (red), the predicted
522 trajectory by our model (blue) and persistence trajectory (green) at (a) week-1, (c)
523 week-2. (b), (d) are the same as (a) and (c), respectively, but for a recurved trajectory.
524 The biweekly eddy positions on each trajectory are shown by the solid circles.
525

Ocean Sci. Discuss., https://doi.org/10.5194/os-2018-116
Manuscript under review for journal Ocean Sci.
Discussion started: 1 November 2018

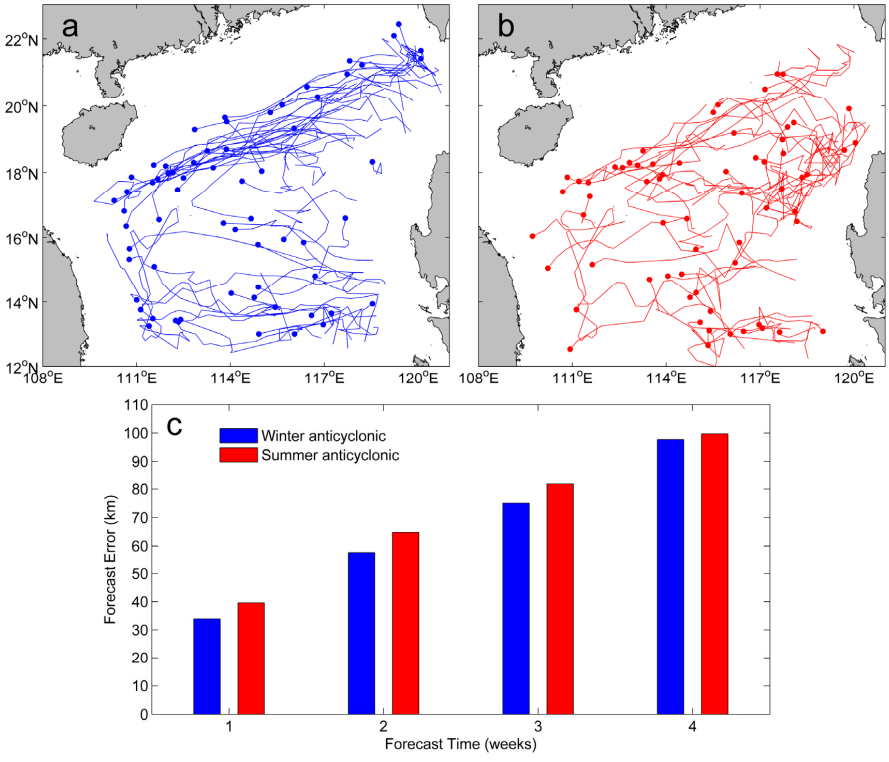

Figure 6. The trajectories of anticyclonic eddies in (a) winter and (b) summer with lifetime ≥ 5 weeks in the South China Sea (SCS). The solid circle represents the ending position of each trajectory. (c) Comparison of their mean forecast errors over a 4-week window.

Ocean Sci. Discuss., https://doi.org/10.5194/os-2018-116
Manuscript under review for journal Ocean Sci.
Discussion started: 1 November 2018

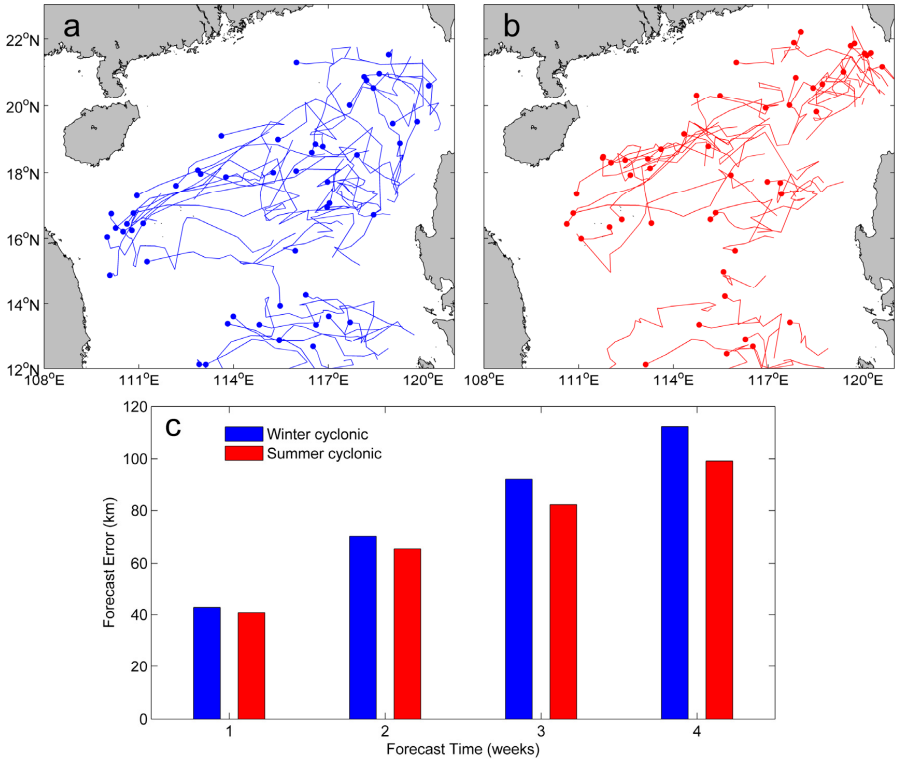

Figure 7. The same as Fig. 6, but for the cyclonic eddies.

Ocean Sci. Discuss., https://doi.org/10.5194/os-2018-116
Manuscript under review for journal Ocean Sci.
Discussion started: 1 November 2018

537 **Table 1.** The Eight Predictors Used in the Predictive Model

538

NO	Predictor	Description
1	LON	Initial longitude
2	LAT	Initial latitude
3	U_PAST	Eddy zonal motion past 1-week
4	V_PAST	Eddy meridional motion past 1-week
5	U_CLIM	Climatological eddy zonal motion from MCC
6	V_CLIM	Climatological eddy meridional motion from MCC
7	U_ADT	Initial zonal absolute geostrophic flow
8	V_ADT	Initial meridional absolute geostrophic flow

539

Ocean Sci. Discuss., https://doi.org/10.5194/os-2018-116
Manuscript under review for journal Ocean Sci.
Discussion started: 1 November 2018

540 **Table 2.** Normalized Regression Coefficients for Use with the Eddy Zonal (Meridional) Motion

541 Prediction Equation

542

NO	Predictor	1 week	2 weeks	3 weeks	4 weeks
1	LON	-0.10 (0.03)	-0.14 (0.04)	-0.18 (0.05)	-0.24 (0.06)
2	LAT	0.10 (0.02)	0.13 (0.01)	0.16 (0.00)	0.18 (-0.03)
3	U_PAST	0.26 (0.00)	0.21 (0.03)	0.19 (0.07)	0.18 (0.09)
4	V_PAST	-0.02 (0.19)	-0.01 (0.10)	0.01 (0.08)	0.00 (0.08)
5	U_CLIM	0.14 (0.09)	0.19 (0.13)	0.23 (0.16)	0.26 (0.16)
6	V_CLIM	0.05 (0.17)	0.07 (0.23)	0.09 (0.26)	0.16 (0.27)
7	U_ADT	-0.05 (0.02)	-0.07 (0.02)	-0.07 (0.02)	-0.07 (0.03)
8	V_ADT	-0.03 (-0.07)	-0.01 (-0.08)	0.02 (-0.09)	0.04 (-0.09)

Ocean Sci. Discuss., https://doi.org/10.5194/os-2018-116
Manuscript under review for journal Ocean Sci.
Discussion started: 1 November 2018

543 **Table 3.** Statistics of our Predictive Model for Different Forecast Time of Eddy Propagation Positions in Terms of Longitudes (Latitudes)
544

Forecast weeks	Total (Predicted) Number of Points	RMSE, degrees	Correlation Coefficient	Mean Distance Error, km	Mean Distance Error From Persistence, km
1	2604 (623)	0.33 (0.30)	0.99 (0.99)	38.1	47.6
2	2310(549)	0.55 (0.47)	0.97 (0.98)	64.8	95.2
3	2016 (475)	0.72 (0.61)	0.95 (0.97)	86.6	135.0
4	1722 (401)	0.89 (0.73)	0.93 (0.95)	106.5	180.5

545